

RSC Advances



This is an *Accepted Manuscript*, which has been through the Royal Society of Chemistry peer review process and has been accepted for publication.

Accepted Manuscripts are published online shortly after acceptance, before technical editing, formatting and proof reading. Using this free service, authors can make their results available to the community, in citable form, before we publish the edited article. This *Accepted Manuscript* will be replaced by the edited, formatted and paginated article as soon as this is available.

You can find more information about *Accepted Manuscripts* in the [Information for Authors](#).

Please note that technical editing may introduce minor changes to the text and/or graphics, which may alter content. The journal's standard [Terms & Conditions](#) and the [Ethical guidelines](#) still apply. In no event shall the Royal Society of Chemistry be held responsible for any errors or omissions in this *Accepted Manuscript* or any consequences arising from the use of any information it contains.

ARTICLE

Synthesis and Characterization of [60]Fullerene-poly(3-azidomethyl-3-methyl oxetane) and Its Thermal Decomposition

Cite this: DOI: 10.1039/x0xx00000x

Jun Zhao,^a Bo Jin,^{a,*} Rufang Peng,^{a,*} Nengmei Deng,^a Wenlin Gong,^a Qiangqiang Liu,^a Shijin Chu^aReceived 00th January 2012,
Accepted 00th January 2012

DOI: 10.1039/x0xx00000x

www.rsc.org/

A new functionalized fullerene derivative [60]fullerene poly(3-azidomethyl-3-methyl oxetane) (C₆₀-PAMMO) was synthesized for the first time using a modified Bingel reaction of [60]fullerene (C₆₀) and bromomalonic acid poly(3-azidomethyl-3-methyl oxetane) ester (BM-PAMMO). The product was characterized by Fourier transform infrared (FTIR), ultraviolet-visible (UV-vis), and nuclear magnetic resonance (NMR) spectroscopy analyses. Results confirmed the successful preparation of C₆₀-PAMMO. Moreover, the thermal decomposition of C₆₀-PAMMO was analyzed by differential scanning calorimetry (DSC), thermogravimetric analysis coupled with infrared spectroscopy (TG-IR), and in situ FTIR. C₆₀-PAMMO decomposition showed a three-step thermal process. The first step at approximately 150 °C was related to the cycloaddition of azido groups (-N₃) with [60]fullerene. The second step was ascribed to the remainder decomposition of the PAMMO main chain at approximately 230 °C. The final step was attributed to the burning decomposition of amorphous carbon, the main chain, *N*-heterocyclic and carbon cage at around 510 °C.

Introduction

Given the attractive chemical and physical properties of C₆₀, studies on its application are extensive since its macroscale synthesis,¹ which shows promising applications in medicine and material science. As C₆₀ has good features such as thermal stability, antioxidation, etching resistance, good compatibility with propellant components, and beneficial for preventing aging.²⁻⁵ Thus, C₆₀ can replace carbon black as the solid rocket fuel additive that can increase the burning rate and combustion catalytic efficiency and decrease the amount of NO_x in the exhaust gas.⁶⁻¹¹ If some energetic groups, such as nitro group (-NO₂) and azido group (-N₃), were incorporated in the [60]fullerene cage, then a better fuel additive may be obtained.¹²⁻²⁶

Usually, azide energetic material has higher thermal stability²⁷⁻³³ and the thermal decomposition of azido group was ahead of the main chain and independent, which can help increase the energy and accelerate the decomposition of the propellant. Poly(3-azidomethyl-3-methyl oxetane) (PAMMO), a azido polymer, has attracted researchers' attention and has been used as energetic binder in propellant and explosive formulations because of its higher positive heat of formation, higher density, higher nitrogen content, and lower mechanical sensitivity.³⁴⁻³⁹ Moreover, the terminal hydroxyl group of PAMMO can be easily modified through various reactions, such as esterification, acetalization, etherification, *etc.*^{40,41} In this paper,

PAMMO was further functionalized *via* esterification with malonyl dichloride and subsequent brominate reaction to afford bromomalonic acid PAMMO ester (BM-PAMMO). BM-PAMMO easily reacts with C₆₀ through a modified Bingel reaction⁴² to afford an energetic fullerene derivative C₆₀-PAMMO. The thermal decomposition performance and decomposition mechanism of C₆₀-PAMMO were also examined in detail.

Experimental section

Chemicals and Apparatus

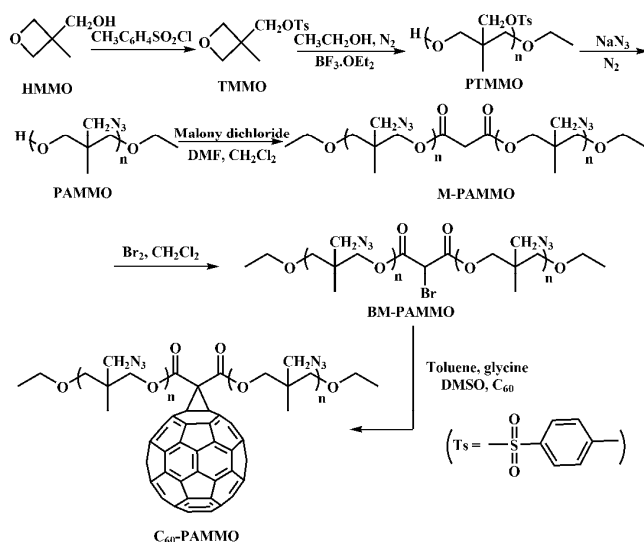
[60]fullerene was purchased from Henan Tianan Company. HMMO was purchased from Xiya Reagent. The 300-400 mesh silica gel was purchased from Qingdao Hailang. All the other chemicals were purchased from Chengdu Kelong Chemical Reagents Company. Dichloromethane was dried on P₂O₅ and redistilled under vacuum before use. *N,N*-dimethylformamide (DMF) and dimethyl sulfoxide (DMSO) were dried on anhydrous MgSO₄ and distilled under vacuum.

¹H and ¹³C NMR spectra were recorded on a Bruker Advance DRX 400-MHz instrument with CDCl₃ as the solvent and tetramethylsilane as the internal reference. FTIR spectra were obtained on a Nicolet 6700 FT-IR spectrometer with a resolution of 4 cm⁻¹ from 400 cm⁻¹ to 4000 cm⁻¹. UV-vis spectra were recorded on UNICON UV-2102 PCS spectrometer with CH₂Cl₂ as the solvent. Differential scanning calorimetry (DSC) curves were

recorded on a SDT Q600 TGA-DSC instrument in flowing air at a heating rate of 10 °C/min. Thermogravimetry with infrared spectrometry (TG-IR) was performed using a Q500 thermogravimetric analysis (TGA) instrument in air at a heating rate of 10 °C/min. The molecular weights and the polydispersity index were obtained with gel permeation chromatography (GPC; LC-20A, Shimadzu) and the mobile phase was tetrahydrofuran (1.0 mL/min). The hydroxyl value (OHV) of PAMMO was determined by the acetic anhydride acetylation method.⁴³

Synthesis

[60]Fullerene-poly(3-azidomethyl-3-methyl oxetane) (C₆₀-PAMMO) was synthesized in six steps, as shown in Scheme 1. First, Ts protected 3-hydroxymethyl-3-methyl oxetane (TMMO) was obtained *via* the reaction of 3-hydroxymethyl-3-methyl oxetane and tosyl chloride. With the use of BF₃•OEt₂ as catalyst and ethanol as initiator, TMMO was polymerized to produce monoethyl-terminated PTMMO. The azide substitution of PTMMO resulted to afford the monoethyl-terminated PAMMO. BM-PAMMO was synthesized by esterifying and then brominating of PAMMO and malonyl dichloride. Finally, BM-PAMMO was allowed to react with C₆₀ through a modified Bingel reaction to get C₆₀-PAMMO.



Scheme 1. Synthesis route of C₆₀-PAMMO.

Synthesis of TMMO.

20.97 g Tosyl chloride (0.11 mol) dissolved in 40 mL pyridine was added slowly into a flask containing 10.20 g 3-hydroxymethyl-3-methyl oxetane (0.10 mol). The mixture was reacted at -5 °C for 0.5 h under nitrogen atmosphere and then reacted at room temperature for 12 h. The mixture was filtered and the filtrate was added slowly into a vigorously stirred mixture of deionized water (200 mL) and crushed ice, which was maintained under stirring for another 2 h. A white precipitate appeared and was collected, washed with cold water thrice, and dried under vacuum to obtain a white powder of product (18.20 g, corresponding to a yield of 71.1%). Elemental analysis (EA): Found/%: C, 58.54; H, 5.85; S, 12.48. Calculated/%: C, 58.47; H, 5.88; S, 12.54. UV-vis (CH₂Cl₂) λ/nm: 205, 211, 237, 262, 273. IR (KBr) ν/cm⁻¹: 2875 (ν_s CH₂), 1598 (ν_{as} C-

C aromatic ring), 1463 (δ CH₂), 1360 (ν_{as} S(=O)₂), 1180 (ν_s S(=O)₂), 1096 (δ_s C-H aromatic ring), 977 (ν_{as} C-O-C oxetane, ν_{as} S-O-C), 837 (ν_s S-O-C), 665 (ω C-H aromatic ring). ¹H-NMR (CDCl₃, 400 MHz) δ/ppm: 7.83-7.38 (4H, m, aromatic ring), 4.39-4.35 (4H, dd, *J* = 16.9, 6.2 Hz, CH₂O oxetanic ring), 4.12 (2H, s, CH₂OTs), 2.47 (3H, s, CH₃ aromatic ring), 1.32 (3H, s, CH₃).

Synthesis of PTMMO.

1.85 g BF₃•OEt₂ (13.02 mmol), 1.20 g absolute ethyl alcohol (26.00 mmol) and 25 mL dry methylene chloride were introduced into a 100 mL three-neck flask equipped with a mechanical stirrer and thermometer. This mixture was stirred for 0.5 h under argon at (0–5) °C. A solution of 10 g TMMO (0.04 mol) in 20 mL methylene chloride was added dropwise to this reaction mixture. The reaction mixture was stirred at (0–5) °C for 18 h, and then the mixture was allowed to reach 35 °C and maintained for 25 h. Thereafter, the reaction was completed by adding 100 mL of saturated NaCl solution. The organic layer was washed with water (200 mL×3) and the mixture of water/methanol, dried over Na₂SO₄, and filtered and evaporated in vacuum to produce 9.70 g of PTMMO, with a yield of 87%. UV-vis (CH₂Cl₂) λ/nm: 236, 262, 273. IR (KBr) ν/cm⁻¹: 2878 (ν_s CH₂), 1598 (ν_{as} C-C aromatic ring), 1460 (δ CH₂), 1358 (ν_{as} S(=O)₂), 1176 (ν_s S(=O)₂), 1098 (δ_s C-H aromatic ring), 966 (ν_{as} C-O-C, ν_{as} S-O-C), 833 (ν_s S-O-C), 666 (ω C-H aromatic ring). ¹H NMR (CDCl₃, 400 MHz) δ/ppm: 7.76–7.34 (4H, dd, *J* = 12.8, 7.8 Hz, aromatic ring), 3.79 (2H, s, CH₂OTs), 3.43-3.11 (2H, q, *J* = 10.0, 6.3 Hz, CH₂ ethyl), 3.07 (2H, s, CH₂O main chain), 2.43 (3H, s, CH₃ aromatic ring), 1.09-1.06 (3H, t, *J* = 4.8 Hz, CH₃ ethyl), 0.75 (3H, s, CH₃). Molecular Weight (by GPC): *M*_w=1534, *M*_n=1225, *M*_w/*M*_n=1.25.

Synthesis of PAMMO.

6.0 g NaN₃, 18.0 g PTMMO and 30 mL DMSO were introduced into a 100 mL three-neck flask equipped with a mechanical stirrer and thermometer. The reaction mixture was stirred under 100 °C for 120 h. Thereafter, the reaction solution was poured into 200 mL distilled water and extracted with dichloromethane (50 mL×3). The organic layer was washed with distilled water (200 mL×3), dried over Na₂SO₄, and filtered and evaporated in vacuum to produce 6.6 g of PAMMO, with a yield of 83%. UV-vis (CH₂Cl₂) λ/nm: 236, 284. IR (KBr) ν/cm⁻¹: 2972 (ν_{as} CH₂), 2876 (ν_s CH₂), 2102 (ν_{as} N₃), 1282 (ν_s N₃), 1455 (ν CH₂), 1378 (δ_s CH₃), 1355 (ν CH₂), 1111 (ν_{as} C-O-C). ¹H-NMR (CDCl₃, 400 MHz) δ/ppm: 0.94 (3H, s, CH₃ side chain), 1.14-1.22 (3H, t, *J* = 7.0 Hz, CH₃ ethyl), 3.21 (4H, m, CH₂O), 3.26 (2H, s, CH₂N₃), 3.69-3.33 (2H, q, *J* = 18.1 Hz, CH₂ ethyl). ¹³C-NMR (CDCl₃, 100 MHz) δ/ppm: 75.68 (-CH₂O-), 68.36 (HOCH), 67.07 (-CH₂CH₃), 55.53 (N₃CH₂CCH₃), 40.80 (N₃CH₂CCH₃), 18.06 (-CH₂N₃), 14.99 (-CH₃). Molecular weight (by GPC): *M*_w=1027, *M*_n=718, *M*_w/*M*_n=1.43. The hydroxyl equivalent weight was 80.07 mg/g.

Synthesis of M-PAMMO.

0.25 mL of malonyl chloride (2.63 mmol) in 10 mL of dry CH₂Cl₂ was added dropwise to a stirred solution of 2.80 g of PAMMO (4.0 mmol hydroxyl group) and 0.60 mL DMF (7.78 mmol) in 25 mL dry CH₂Cl₂ under Ar atmosphere in an ice bath, and the duration of this

process was more than 30 min. The reaction mixture was stirred at room temperature for 11 h and washed repeatedly with deionized water to neutral. The organic layer was dried with anhydrous MgSO_4 , filtered, and evaporated in vacuum to afford 2.0 g of brown M-PAMMO, with a yield of 66%. UV-vis (CH_2Cl_2) λ/nm : 235, 335. IR (KBr) ν/cm^{-1} : 2974 ($\nu_{\text{as}} \text{CH}_2$), 2877 ($\nu_{\text{s}} \text{CH}_2$), 2102 ($\nu_{\text{as}} \text{N}_3$), 1740 ($\nu \text{C}=\text{O}$), 1279 ($\nu_{\text{s}} \text{N}_3$), 1456 (νCH_2), 1377 ($\delta_{\text{s}} \text{CH}_3$), 1353 (νCH_2), 1112 ($\nu_{\text{as}} \text{C}-\text{O}-\text{C}$). $^1\text{H-NMR}$ (CDCl_3 , 400 MHz) δ/ppm : 0.94 (3H, s, CH_3 side chain), 1.14-1.22 (3H, t, $J = 7.0$ Hz, CH_3 ethyl), 3.21 (4H, m, CH_2O), 3.26 (2H, s, CH_2N_3), 3.69-3.33 (2H, q, $J = 5.3$ Hz, CH_2 ethyl), 3.33 (2H, s, COCH_2CO). $^{13}\text{C-NMR}$ (CDCl_3 , 100 MHz) δ/ppm : 166.17 ($-\text{CH}_2\text{COCH}_2-$), 76.03 ($\text{HOCH}-$), 68.85 ($-\text{CCH}_2\text{CH}_2-$), 66.82 ($-\text{CH}_2\text{CH}_3$), 55.56 ($-\text{CH}_2\text{N}_3$), 41.58 ($\text{N}_3\text{CH}_2\text{CCH}_3$), 41.44 ($-\text{COCH}_2\text{CO}-$), 21.62 ($-\text{CCH}_3$), 15.01 ($-\text{CH}_3$). Molecular weight (by GPC): $M_w=2082$, $M_n=1520$, $M_w/M_n=1.37$.

Synthesis of BM-PAMMO.

0.13 mL of Br_2 (2.54 mmol) in 10 mL of dry CH_2Cl_2 was added dropwise to a stirred solution of 3.1 g of M-PAMMO in 45 mL dry CH_2Cl_2 at room temperature. Then the reaction mixture was stirred at room temperature for 6 h. The reaction was terminated by adding saturated NaBr solution. The mixture was washed with water until the pH was neutral to obtain 2.9 g of BM-PAMMO, with a yield of 85%. UV-vis (CH_2Cl_2) λ/nm (log ϵ): 235 (4.89), 339 (3.98). IR (KBr) ν/cm^{-1} : 2973 ($\nu_{\text{as}} \text{CH}_2$), 2877 ($\nu_{\text{s}} \text{CH}_2$), 2102 ($\nu_{\text{as}} \text{N}_3$), 1740 ($\nu \text{C}=\text{O}$), 1279 ($\nu_{\text{s}} \text{N}_3$), 1455 (νCH_2), 1377 ($\delta_{\text{s}} \text{CH}_3$), 1112 ($\nu_{\text{as}} \text{C}-\text{O}-\text{C}$), 604 ($\nu \text{C}-\text{Br}$). $^1\text{H-NMR}$ (CDCl_3 , 400 MHz) δ/ppm : 0.94 (3H, s, CH_3 side chain), 1.14-1.22 (3H, t, $J = 7.0$ Hz, CH_3 ethyl), 3.21 (4H, m, CH_2O), 3.26 (2H, s, CH_2N_3), 3.61-3.33 (2H, q, $J = 6.4$ Hz, CH_2 ethyl), 5.54 (1H, s, CHBr). $^{13}\text{C-NMR}$ (CDCl_3 , 100 MHz) δ/ppm : 166.17 ($-\text{CH}_2\text{COCH}_2-$), 76.03 ($\text{HOCH}-$), 68.85 ($-\text{CCH}_2\text{CH}_2-$), 66.82 ($-\text{CH}_2\text{CH}_3$), 55.56 ($-\text{CH}_2\text{N}_3$), 41.83 ($-\text{COCHBrCO}-$), 41.58 ($\text{N}_3\text{CH}_2\text{CCH}_3$), 21.62 ($-\text{CCH}_3$), 15.01 ($-\text{CH}_3$). Molecular weight (by GPC): $M_w=2157$, $M_n=1586$, $M_w/M_n=1.36$.

Synthesis of C_{60} -PAMMO.

0.89 g C_{60} (1.24 mmol) and 0.556 g glycine (7.41 mmol) were dissolved in 250 mL of chlorobenzene and 100 mL of DMSO by using ultrasonic irradiation method. Thereafter, 1.21 g of BM-PAMMO was added to the above solution. The mixture was stirred at room temperature for 12 h, and then the resulting solution was repeatedly washed with distilled water to remove DMSO and glycine. Chlorobenzene was then removed under vacuum. The residue was separated on a silica gel column through carbon disulfide and CH_2Cl_2 /ethyl acetate (1:2) as the eluent to obtain 44.30 mg unreacted C_{60} and 1.58 g of C_{60} -PAMMO, with a yield of 87% (based on the consumption of C_{60}). UV-vis (CH_2Cl_2) λ/nm (log ϵ): 235 (4.85), 258 (4.86), 330 (4.35), 435 (3.22). IR (KBr) ν/cm^{-1} : 2965 ($\nu_{\text{as}} \text{CH}_2$), 2856 ($\nu_{\text{s}} \text{CH}_2$), 2096 ($\nu_{\text{as}} \text{N}_3$), 1736 ($\nu \text{C}=\text{O}$), 1262 ($\nu_{\text{s}} \text{N}_3$), 1456 (νCH_2), 1384 ($\delta_{\text{s}} \text{CH}_3$), 1171 (C_{60} specific absorbing peak), 1103 ($\nu_{\text{as}} \text{C}-\text{O}-\text{C}$), 526 (C_{60} specific absorbing peak). $^1\text{H-NMR}$ (CDCl_3 , 400 MHz) δ/ppm : 0.87 (3H, s, CH_3 side chain), 1.16-1.08 (3H, t, CH_3 ethyl), 3.15 (4H, m, CH_2O), 3.19 (2H, s, CH_2N_3), 3.61-3.33 (2H, q, CH_2 ethyl). Molecular weight (by GPC): $M_w=3255$, $M_n=2276$, $M_w/M_n=1.43$.

Results and discussion

Characterization of C_{60} -PAMMO.

The structure of C_{60} -PAMMO was confirmed by FT-IR, UV-vis, ^1H NMR, and ^{13}C NMR spectral analyses. The UV-vis spectra of BM-PAMMO and C_{60} -PAMMO are presented in Figure 1. As shown in Figure 1, the UV-vis spectrum of BM-PAMMO shows an absorption peak at 235 nm, which is ascribed to the $\pi \rightarrow \pi^*$ transition of the $-\text{N}_3$ group. The UV-vis spectrum of C_{60} -PAMMO also shows a sharp absorption peak at approximately 235 nm, which implies the presence of $-\text{N}_3$ group in C_{60} -PAMMO. Moreover, compared with BM-PAMMO, three new absorption peaks at 258, 330 and 435 nm are observed in the UV-vis spectrum of C_{60} -PAMMO. The peaks at 258 and 330 nm are the characteristic absorption of the skeleton structure of C_{60} , and the weak absorption band at 435 nm is typical of monoadducts at the closed 6,6-junction of C_{60} .^{44,45}

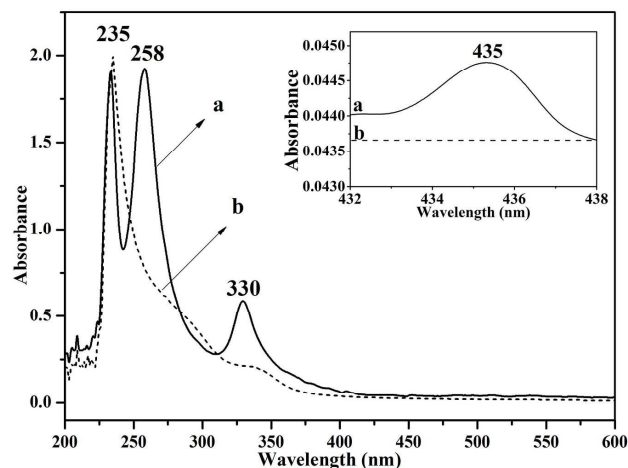


Figure 1. UV-vis absorption spectrum of BM-PAMMO and C_{60} -PAMMO. (a) C_{60} -PAMMO and (b) BM-PAMMO

Figure 2 shows the FTIR spectra of BM-PAMMO and C_{60} -PAMMO. As shown in Figure 2(b), in the FTIR spectra of BM-PAMMO, the peak at 1740 cm^{-1} can be assigned to the $\text{C}=\text{O}$ stretching vibration, and the peaks at 1112 cm^{-1} and 1279 cm^{-1} correspond to the $\text{C}-\text{O}-\text{C}$ symmetric and antisymmetric stretching vibrations. The strong absorption peak at 2102 cm^{-1} corresponds to the $-\text{N}_3$ group of PAMMO, and the peaks at 2973 , 2934 and 2877 cm^{-1} are ascribed to the $\text{C}-\text{H}$ symmetric and antisymmetric stretching vibrations of PAMMO respectively.³⁹ The peak at 604 cm^{-1} is due to the $\text{C}-\text{Br}$ stretching vibration. Compared with BM-PAMMO (Figure 2(b)), the $\text{C}-\text{Br}$ stretching vibration peak disappeared in Figure 2(a). In addition, the new peaks in Figure 2(a) at 526 cm^{-1} and 1171 cm^{-1} are the characteristic absorption peaks of C_{60} cage.⁴⁶

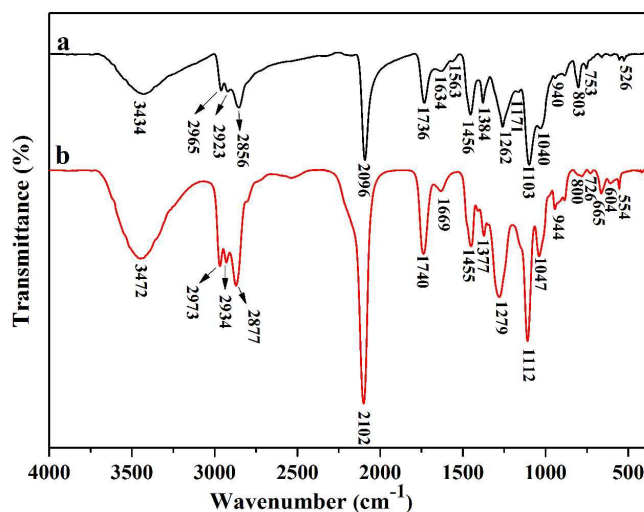


Figure 2. ATR-FTIR absorption spectra of BM-PAMMO and C₆₀-PAMMO. (a) C₆₀-PAMMO and (b) BM-PAMMO.

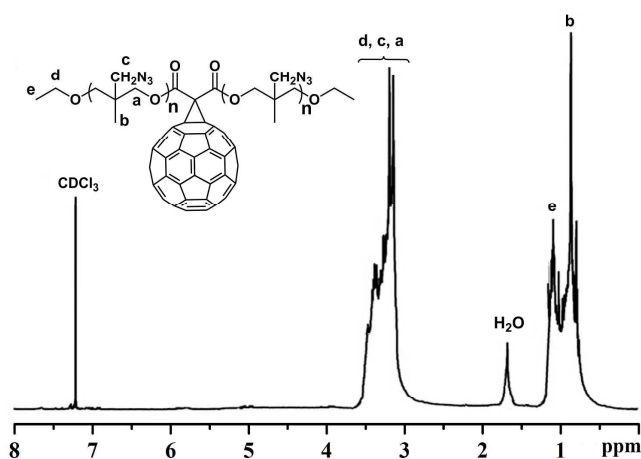


Figure 3. ¹H NMR spectrum of C₆₀-PAMMO.

The ¹H NMR spectrum also confirmed the successful introduction of PAMMO to C₆₀ cage. Figure 3 shows the ¹H NMR spectrum of C₆₀-PAMMO. As shown in Figure 3, the peaks at around 3.10 and 3.60 ppm are attributed to the methylene protons of the main chain -CH₂O- protons (denoted a and d) and the methylene protons of the side chain -CH₂N₃ protons (denoted c). The methyl protons of the CCH₃ (denoted b) and CH₃CH₂O- (denoted e) appear at 0.75-1.20 ppm.

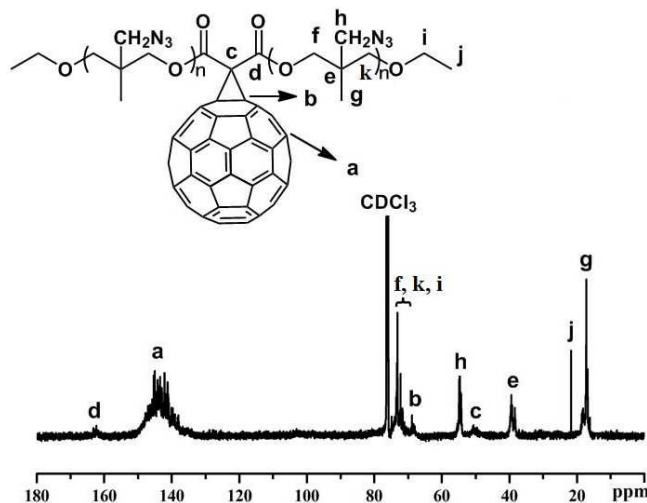


Figure 4. ¹³C NMR spectrum of C₆₀-PAMMO.

The ¹³C NMR spectrum of C₆₀-PAMMO is presented in Figure 4. The signals of the carbonyl carbon (-C=O, denoted d) and the quaternary carbon bounding to C₆₀ (denoted c) appear at $\delta = 162.20$ – 163.00 ppm and $\delta = 50.20$ ppm, respectively.⁴⁷ The signals at around 74.00 and 71.20 ppm are attributed to the methylene carbons of the main chain -CH₂O- group (denoted f, k and i). The signals from 54.22 ppm to 52.34 ppm are attributed to the azidomethyl carbon of the side chain -CH₂N₃ group (denoted h). The quaternary carbon (denoted e) of the main chain appears at around 39.52 ppm. The methyl carbons of the side chain (denoted g) and terminal CH₃CH₂O- group (denoted j) appear at around 16.68 ppm and 20.89 ppm respectively. The two sp³-carbons of the C₆₀ cage (denoted b) appear at 68.34 ppm, and 58 sp²-carbons of fullerene cage (denoted a) overlap and appear from 150.00 ppm to 135.40 ppm as a broad peak.⁴⁸

Thermal analysis

The thermal stability of energetic materials has an important effect on the preparation, storage, processing, and application scope. Thus, DSC and TGA methods were adopted to evaluate the decomposition behavior of C₆₀-PAMMO.

The DSC curve of C₆₀-PAMMO under air atmosphere is showed in Figure 5. Three exothermic peaks were observed from 100 °C to 600 °C. The first exothermic peak under atmosphere at 157 °C is probably caused by the initial intramolecular or intermolecular reaction of the -N₃ group and fullerene carbon cage.⁴⁹ The second exothermic peak at 324 °C is due to the decomposition of PAMMO main chain. The third peak at 513 °C can be attributed to the decomposition of the C₆₀ skeleton. In addition, the decomposition enthalpies of the three exothermic peaks are 39 J/g, 2858 J/g and 1005 J/g respectively.

In order to well understand the thermal decomposition mechanism of C₆₀-PAMMO, thermogravimetric analysis tandem infrared spectrum (TGA-IR) was used to rapidly identify the constituents of the thermal decomposition gas (Figure 6). As shown in Figure 6(a), the TGA and DTG curves show the three-step thermal degradation

of C₆₀-PAMMO under air atmosphere. The first thermal degradation appears at 148 °C, with around 10.36% weight loss. Thereafter, two thermal degradations appear at 323 °C and 512 °C with approximately 35.99% and 51.91% weight losses, respectively. Figure 6(b) shows the IR spectra of the thermal decomposition gas of C₆₀-PAMMO at 323 °C and 512 °C, respectively. As depicted in Figure 6(a), the decomposed products of C₆₀-PAMMO at 323 °C under air atmosphere are mainly CO₂ (2310 and 2367 cm⁻¹), CO (2185 and 2110 cm⁻¹) and C=O (1749 cm⁻¹), and the decomposed products at 512 °C under air atmosphere are mainly CO₂ (2302 and 2364 cm⁻¹), CO (2109 and 2177 cm⁻¹), N₂O (2247 cm⁻¹) and H₂O (3543 cm⁻¹). Obviously, these results are different from the previously reported that the thermal degradation of azide polymer appears at around 200 °C, and the main gas products are CO, HCN, HCHO and NH₃. Thus, these results indicate that the first thermal degradation of C₆₀-PAMMO at 148 °C is probably due to the decomposition of the -N₃ group, and decomposition mechanism is probably through the initial intramolecular or intermolecular cycloaddition of -N₃ and fullerene carbon cage and subsequent decomposition to release nitrogen (Scheme 2).

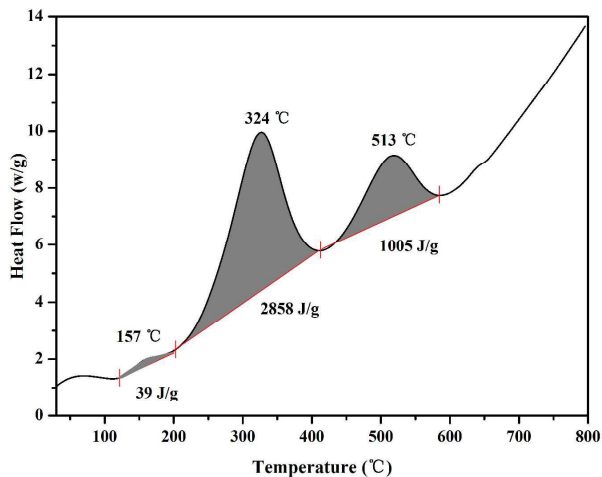


Figure 5. DSC curve of C₆₀-PAMMO under air atmosphere.

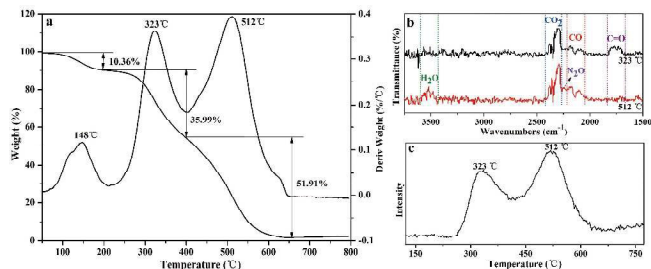
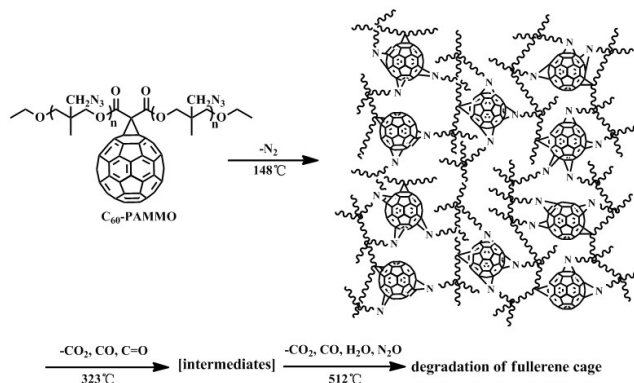


Figure 7. (a) TGA and DTG curves of C₆₀-PAMMO under atmosphere; (b) IR spectrum of the thermal decomposition gas of C₆₀-PAMMO at 323 °C and 512 °C under atmosphere; (c) Thermal decomposition gas intensity under different temperature.



Scheme 2. The decomposition mechanism of C₆₀-PAMMO.

In order to demonstrate this decomposition mechanism, in situ FTIR was used to rapidly identify the constituents of decomposition condensed-phase residue. Figure 7(a) shows the infrared spectra of C₆₀-PAMMO decomposition condensed-phase residue at 27 °C, 127 °C, 152 °C, 172 °C, 207 °C and 262 °C under air atmosphere, respectively. Figure 7 (b) shows the infrared absorption intensity ratio of -N₃ ($\nu = 2096$ cm⁻¹) and C=O ($\nu = 1736$ cm⁻¹), C₆₀ ($\nu = 526$ cm⁻¹) and C=O ($\nu = 1736$ cm⁻¹) in C₆₀-PAMMO decomposition condensed-phase FTIR spectra at specified temperatures. As shown in Figure 7, both the infrared absorption intensity ratio of -N₃ ($\nu = 2096$ cm⁻¹) and C=O ($\nu = 1736$ cm⁻¹) ($A_{-N_3}/A_{C=O}$) and the infrared absorption intensity ratio of C₆₀ ($\nu = 526$ cm⁻¹) and C=O ($\nu = 1736$ cm⁻¹) ($A_{C_{60}}/A_{C=O}$) were rapidly decreased at 148 °C. The decrease of $A_{-N_3}/A_{C=O}$ shows that the -N₃ started rapid decomposition at 148 °C, and the reduction of $A_{C_{60}}/A_{C=O}$ at 148 °C indicates that the decomposition of -N₃ group is accompanied with the damage of fullerene conjugated structure. Thus, in situ FTIR analytical results strictly corroborate the TGA-IR analyses that C₆₀-PAMMO decomposition at 148 °C is through the initial intramolecular or intermolecular reaction of -N₃ and the fullerene carbon cage.

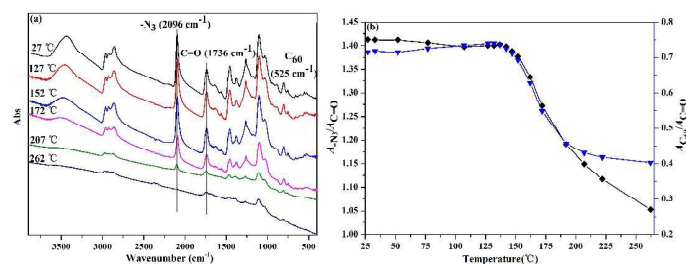


Figure 8. (a) IR spectra of the thermal decomposition remaining solid of C₆₀-PAMMO at 27, 127, 152, 172, 207 and 262 °C respectively; (b) Ratio of the IR absorption peak of -N₃ ($\nu = 2096$ cm⁻¹)/-COO- ($\nu = 1736$ cm⁻¹) and C₆₀ ($\nu = 526$ cm⁻¹)/C=O ($\nu = 1736$ cm⁻¹) at different temperatures.

Conclusions

A new energetic polymer, [60]fullerene-poly(3-azidomethyl-3-methyl oxetane) has been successfully synthesized through the

Bingel reaction of BM-PAMMO and C₆₀. Its structure was systematically characterized by FTIR, UV-vis, ¹H NMR and ¹³C NMR spectroscopy analyses. The thermal stability and thermal decomposition mechanism of [60]fullerene-poly(3-azidomethyl-3-methyl oxetane) was analyzed by DSC, TGA-FTIR, and in situ FTIR. The results showed that the initial decomposition of [60]fullerene-poly(3-azidomethyl-3-methyl oxetane) at 148 °C could be ascribed to the intramolecular or intermolecular reaction of the -N₃ group and fullerene carbon cage.

Acknowledgements

We are grateful for financial support from the National Natural Science Foundation of China (Project No. 21301142, 51372211), National Defense Fundamental Research Projects (Project No. A3120133002), Applied Basic Research Program of Sichuan Province (2014JY0170) and Southwest University of Science and Technology Researching Project (13zx9107, 13zxfk09, 14tdfk05).

Notes and references

^a(State Key Laboratory Cultivation Base for Non-metal Composites and Functional Materials, Southwest University of Science and Technology, Mianyang 621010, P, R, China)

Email: jinbo0428@163.com rfpeng2006@163.com

Electronic Supplementary Information (ESI) available: [details of any supplementary information available should be included here]. See DOI: 10.1039/b000000x/

- 1 H. W. Kroto, A. W. Allaf and S. P. Balm, *Chem. Rev.*, 1991, **91**, 1213-1235.
- 2 P. R. Birkett, *Annu. Rep. Prog. Chem. Sect. A: Inorg. Chem.*, 1999, **95**, 431-451.
- 3 P. A. Troshin and R. N. Lyubovskaya, *Russ. Chem. Rev.*, 2008, **77**, 323-369.
- 4 A. D. Darwish, *Annu. Rep. Prog. Chem. Sect. A: Inorg. Chem.*, 2010, **106**, 356-375.
- 5 M. D. Tzirakis and M. Orfanopoulos, *Chem. Rev.*, 2013, **113**, 5262-5321.
- 6 X. Han, T. F. Wang, Z. K. Lin, D. L. Han, S. F. Li and F. Q. Zhao, *Defence Sci. J.*, 2009, **59**, 284-293.
- 7 T. Heintz, H. Pontius, J. Aniol, C. Birke, K. Leisinger and W. Reinhard, *Propellants Explos. Pyrotech.*, 2009, **34**, 231-238.
- 8 A. J. Bellamy and S. L. Dearing, *Propellants Explos. Pyrotech.*, 2002, **27**, 352-360.
- 9 J. J. Liu, Z. J. Liu, J. Cheng and D. Fang, *J. Solid State Chem.*, 2013, **200**, 43-48.
- 10 H. J. Huang, H. S. Dong, M. Zhang and Y. Xi, *Energ. Mater.*, 2005, **13**, 7-10.
- 11 J. C. Lynch, J. M. Brannon and J. J. Delfino, *J. Chem. Eng. Data.*, 2002, **47**, 542-549.
- 12 S. Tomohiro, H. Ryota, H. Maki and S. Hideo, *Synth. Commun.*, 2014, **44**, 275-279.
- 13 M. Prate, Q. C. Li and F. Wudl, *J. Am. Chem. Soc.*, 1993, **115**, 1148-1150.
- 14 X. H. Dong, W. B. Zhang, Y. W. Li, M. J. Huang, S. Zhang and P. Roderic, *Polym. Chem.*, 2012, **3**, 124-134.
- 15 M. D. Yan, S. X. Cai and F. W. John, *J. Org. Chem.*, 1994, **59**, 5951-5954.
- 16 M. H. Veen, B. Boer, U. Stalmach, K. I. Wetering and G. Hadzioannou, *Macromolecules.*, 2004, **37**, 3673-3684.
- 17 E. Rusen, B. Marculescu, N. Preda and L. Mihut, *J. Polym. Res.*, 2008, **15**, 447-451.
- 18 P. Ravinder and V. Subramanian, *Theor. Chem. Acc.*, 2012, **131**, 1-11.
- 19 M. A. Hiskey, N. Goldman and J. R. Stine, *J. Energ. Mater.*, 1998, **16**, 119-127.
- 20 J. P. Agrawal, *Prog. Energy Combust. Sci.*, 1998, **24**, 1-30.
- 21 M. B. Talawar, R. Sivabalan, T. Mukundan, H. Muthurajan, A. K. Sikder, B. R. Gandhe and A. S. Rao, *J. Hazard. Mater.*, 2009, **161**, 589-607.
- 22 D. M. Badgujar, M. B. Talawar, S. N. Asthana and P. P. Mahulikar, *J. Hazard. Mater.*, 2008, **151**, 289-305.
- 23 A. K. Sikder and S. Nirmala, *J. Hazard. Mater.*, 2004, **112**, 1-15.
- 24 R. Singh, D. Srivastava and S. K. Upadhyay, *Polym. Sci. Ser. B.*, 2012, **54**, 88-93.
- 25 F. Cataldo, O. Ursini and G. Angelini, *Carbon.*, 2013, **62**, 413-421.
- 26 N. X. Wang, *Propellants Explos. Pyrotech.*, 2001, **26**, 109-111.
- 27 B. Jin, J. Shen, R. F. Peng, Y. J. Shu, S. J. Chu and H. S. Dong, *Polym. Degrad. Stab.*, 2012, **97**, 473-480.
- 28 S. Brochu and G. Ampleman, *Macromolecules.*, 1996, **29**, 5539-5545.
- 29 B. Jin, J. Shen, R. F. Peng, Y. J. Shu, S. J. Chu and H. S. Dong, *J. Polym. Res.*, 2012, **19**, 1-9.
- 30 A. M. Kawamoto, U. Barbieri, T. Keicher, H. Krause, J. A. Saboia Holanda, M. Kaiser and G. Polacco, *Propellants Explos. Pyrotech.*, 2008, **33**, 365-372.
- 31 I. K. Varma, V. Choudhary, B. Gaur, B. Lochab, S. Oberoi and R. Chauhan, *J. Appl. Polym. Sci.*, 2006, **101**, 779-786.
- 32 T. M. Klapötke and J. Stierstorfer, *Cent. Eur. J. Energ. Mater.*, 2008, **5**, 13-30.
- 33 Y. M. Mohan and K. M. Raju, *Des. Monomers Polym.*, 2005, **8**, 159-166.
- 34 A. A. Albarran, E. Silantjeva and K. S. Seo, *Polym. Chem.*, 2014, **5**, 4710-4714.
- 35 M. S. Eroğlu and O. Güven, *Polymer.*, 1998, **39**, 173-176.
- 36 P. Sreekumar and H. G. Ang, *Polym. Degrad. Stab.*, 2007, **92**, 1365-1377.
- 37 Y. M. Mohan and K. M. Raju, *Int. J. Polym. Mater.*, 2006, **55**, 203-217.
- 38 X. N. Zhang, G. G. Xu, J. P. Xu and W. M. Wang, *Chin. J. Explos. Propellant.*, 1999, **22**, 33-36.
- 39 U. Barbieri, G. Polacco and E. Paesano, *Propellants Explos. Pyrotech.*, 2006, **31**, 369-375.
- 40 T. Huang, B. Jin, R. F. Peng and S. J. Chu, *Int. J. Polym. Anal. Charact.*, 2014, **19**, 522-531.
- 41 X. Guan, L. Li, J. Zheng and G. Li, *RSC Advance.*, 2011, **1**, 1808-1814.
- 42 B. Jin, J. Shen, R. F. Peng, R. Z. Zheng and S. J. Chu, *Tetrahedron Lett.*, 2014, **55**, 5007-5010.
- 43 M. H. Tavassoli-Kafrani, J. M. Curtis and F. R. van de Voort, *J. Am. Oil Chem. Soc.*, 2014, **91**, 925-933.
- 44 F. Diederich, L. Isaacs and D. Philp, *Chem. Soc. Rev.*, 1994, **23**, 243-255.
- 45 M. Maggini, G. Scorrano and M. Prato, *J. Am. Chem. Soc.*, 1993, **115**, 9798-9799.
- 46 W. Krätschmer, L. D. Lamb, K. Fostiropoulos, D. R. Huffman, *Nature*, 1990, **347**, 354-358.
- 47 D. Sigwalt, F. Schillinger, S. Guerra, M. Holler, M. Berville and J. F. Nierengarten, *Tetrahedron Lett.*, 2013, **54**, 4241-4244.
- 48 F. Cheng, X. Yang, H. Zhu and Y. Song, *Tetrahedron Lett.*, 2000, **41**, 3947-3950.
- 49 S. González, N. Martín, A. Swartz and D. M. Guldi, *Org. Lett.*, 2003, **5**, 557-560.